Fluctuating Reduction Method for Generation Power of the Wind-PV Hybrid System

Jin-Seok Oh* and Ji-Young Lee**

Abstract - This paper reports the performance of a CB (Circuit Breaker) and converter for the battery operated Wind-PV (Photovoltaic) system. For this purpose, a fluctuating reduction controller for an electric generation hybrid (wind+PV) system is suggested. The method operates a wind turbine, PV, CB, converter and battery. Integration of wind and PV sources, which are generally complementary, usually reduce the capacity of the battery. Also, CB controls the overvoltage of the generation system. The objective is to control the operation of the converter and the CB and reduce power fluctuation. This paper includes discussion on system performance, power quality, fluctuation and effect of the randomness of the wind.

Keywords: circuit breaker, converter, hybrid, fluctuation, photovoltaic, wind

1. Introduction

The wind energy conversion system is based upon the well-known DC link converter. The wind generator provides current at a variable frequency. This current is rectified onto the DC link using a converter with six diodes.

Generally, the wind turbine generation system has to use AC-DC converters for uninterruptible power supply. Fig. 1 shows the schematic diagram of the proposed system for the wind turbine generation which consists of a converter, CB and battery.

The proposed power conversion scheme has a variety of pattern applications in hybrid generation systems.

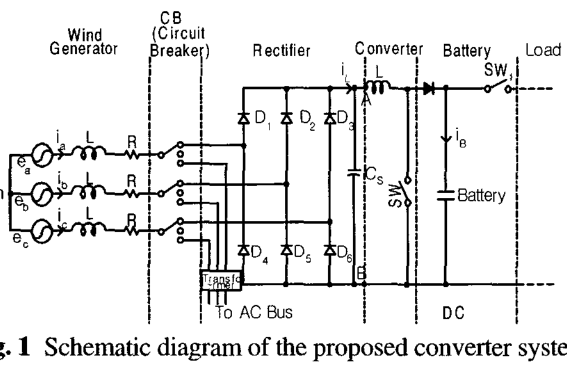

Fig. 1 Schematic diagram of the proposed converter system

It also functions as an AC to DC converter, thus transferring power from the hybrid generator to the battery while the generator supplies power to the converter.

This paper describes the CB control algorithm for overvoltage control and the AC-DC converter algorithm for boosting the generation power as a booster for generation power applications. The algorithm is developed from an understanding of the energy flow within the system. The proposed scheme can also operate as a battery charger and a power supply without the need for any additional power circuit components.

The proposed AC-DC converter with the network is addressed using case studies of voltage fluctuation and harmonics elimination.

In this paper, the impacts on voltage fluctuation can be minimized and furthermore, the network voltage control may also be improved by the proposed operating algorithm.

2. Basic Structure and Operating Principle

The wind generator provides voltage and current at a frequency directly correlating to the operating speed of the wind turbine.

A converter, typically containing six devices, rectifies voltage and current onto the DC link. A capacitor bank provides filtering, resulting in a voltage stiff DC link characteristic.

The proposed power conversion system converts energy from a variable frequency wind-power to a fixed frequency output as shown in Fig. 1. The system consists of a wind generator, rectifier, converter and CB. These elements are discussed below.

2.1 Wind generator

The wind generator is linked to the battery through the

* Division of Mechatronics Engineering, Korea Maritime University, Korea. (ojs@hhu.ac.kr)
** Division of Marine System Engineering, Graduate School of Korea Maritime University, Korea. (hannar52@bada.hhu.ac.kr)
Received October 2, 2003 ; Accepted May 14, 2004

CB and the AC-DC converter. Fig. 1 presents wind generating power load to the bus or AC-DC converter according to the CB condition. The power captured by the wind turbine may be written as equation (1).

$$P_{wt} = 0.5\rho A C_P V^3 \tag{1}$$

where, ρ is air density (kg/m³), A is swept area (m²), C_P is coefficient of wind turbine, V is wind velocity (m/s).

The rotor speed can be described in the following equation:

$$\frac{d\omega_{wm}}{dt} = \frac{1}{J}\int (T_{wa} - T_{wL})dt \tag{2}$$

Where, ω_{wm} is angular shaft speed, J is the inertia, T_{wa} is aerodynamic torque captured from the wind and T_{wL} is the electric torque load. The rotor speed acceleration and deceleration can be described as equation (2). The rate of rotor speed is proportional to the inverse of the inertia and difference between T_{wa} from T_{wL}. The aerodynamic torque is affected by the operating C_P. The voltage fluctuation problem is closer to a steady state problem such as load varying, which is well defined by the real and reactive power distribution.

To understand the effect of fluctuating winds more precisely, consider the theoretical (power/wind speed) curves, for steady winds, represented by the full line in Fig. 2.

As the wind speed fluctuates in the range of the mean value, the power will also fluctuate so that the operating point moves, at varying rates, backwards and forwards along the curve.

When the mean wind speed is near either the cut-in speed or the rated wind speed, the true operating point will lie off the curve. Near cut-in it will lie above the curve and near the rated wind speed it will lie below.

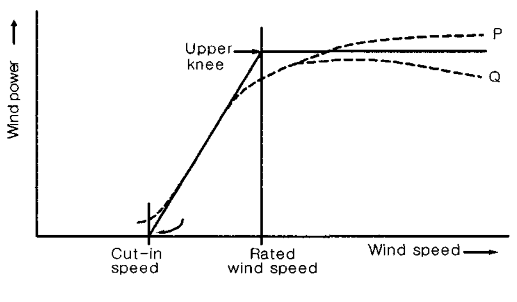

Fig. 2 Relationship between power and wind speed

The power curve in the actual operation will thus be a distortion of the theoretical curve. The amount of the distortion depends upon the amplitude of the wind speed fluctuations. The actual power curve for wind speeds above the rated value may thus lie between the limits indicated by the P-curve and Q-curve in Fig. 2. The characteristics of the wind generator are as follows:

Rated power: 60W, cut-in wind speed: 4m/sec, rated wind speed: 11m/sec, cut-out wind speed: 20m/sec.

The wind speed and power curves are shown in Fig. 3. Fig. 3 illustrates that the generating electric power is in accordance with the wind speed. It is also noted that the varying wind power can result in bus voltage fluctuation.

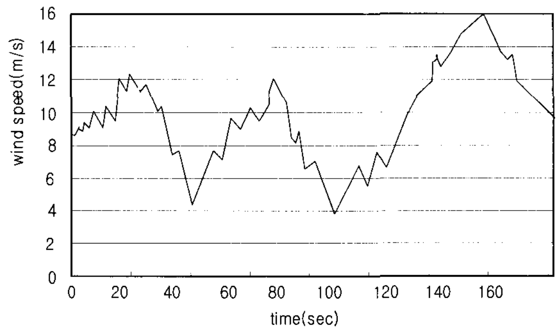

(a) Wind speed

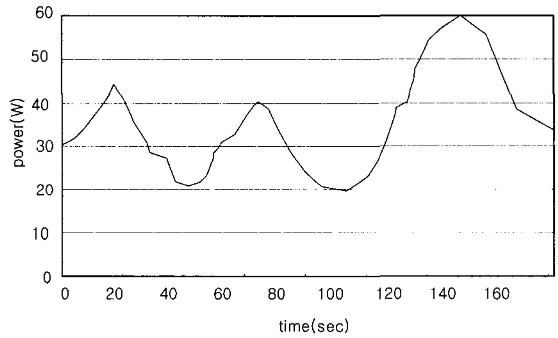

(b) Output power

Fig. 3 Wind speed (a) and Output power (b)

2.2 The PV modules

The PV module manufacturer rating is 60W. The PV module power can be calculated by equation (3)

$$P = I_{ph}V_p - I_o V_p \exp(\frac{q}{KT}V_p - I_o) \tag{3}$$

Where I_{ph} is the cell photo current, V_P is the PV output voltage, I_o is the saturation current, q is the charge of electron, K is Boltzman's constant and T is the cell temperature. The relation between V_P and derivative (dP/dV_p) of output power with respect to output voltage can be expressed as

$$\frac{dP}{dV_p} = I_{ph} - I_o \exp(\frac{q}{KT}V_p)[\exp(-I_o) + \frac{q}{KT}V_p] \tag{4}$$

Fig. 4 shows the characteristic curves of equations (3) and (4), and their relationship.

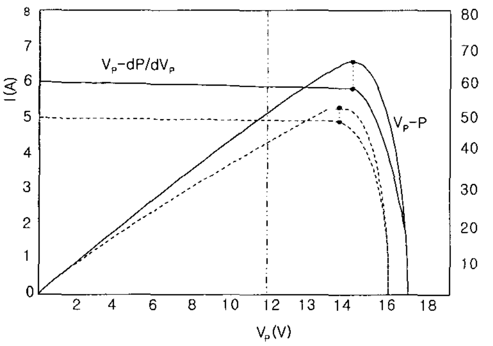

Fig. 4 Characteristic of PV module

It is shown that the MPP (Maximum Power Point) must correspond to such a point where the dP/dV_p is equal to zero. The PV module output voltage can be adjusted by this concept. In this paper, the MPPT is designed by the MPC algorithm with $dP/dV_p = 0$. The PV specifications are as follows:

The open circuit voltage is 20V, rated circuit voltage is 16V, rated current is 5A, and rated power is 60W.

2.3 Converter

The converter regulates the DC output of the wind generator-rectifier unit and PV by switching the ratio controller as demonstrated in Fig. 5.

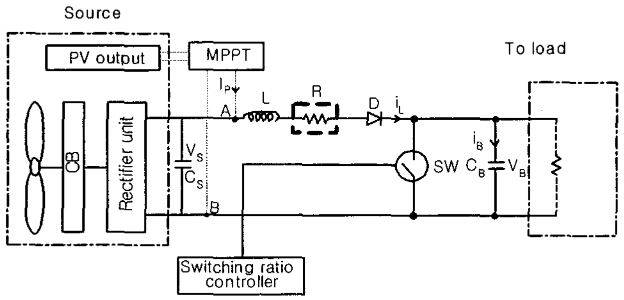

Fig. 5 Block diagram of the generator and converter

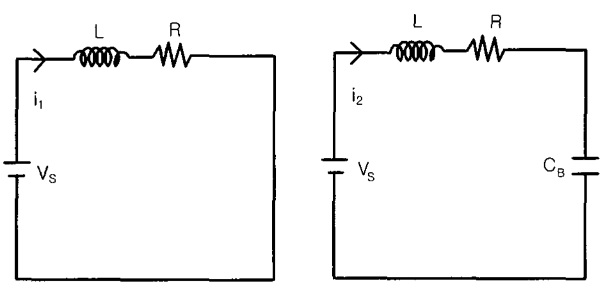

(a) on-state (b) off-state

Fig. 6 Equivalent circuits for the two states

We will suppose that the system switches from one state to another. Its equivalent circuits for on-state and off-state are provided in Fig. 6.

In Fig. 6, the currents i_1 and i_2 are given by

$$i_1 = \frac{V_s}{R}[1-\exp(-t/\tau)] + I_1 \exp(-t/\tau) \tag{5}$$

$$i_2 = \frac{V_s - V_B}{R}[1-\exp(-t/\tau)] + I_2 \exp(-t/\tau) \tag{6}$$

Where τ = L / R is the time constant, and R is the forward resistance of the diode and the equivalent series resistance of the inductor. V_s is the generating voltage, V_B is the battery voltage, and t is the on and off state switching time.

Equations (5) and (6) are valid for T = t_{on} + t_d for continuous current and t_{on} + t_d < T for discontinuous current. T is the switching period and t_d is the time at which the current becomes zero. From equation (6), t_d is as follows;

$$t_d = \tau \cdot \ln[\frac{1 - A\cdot\exp(-t_{on}/\tau)}{1-A}] \tag{7}$$

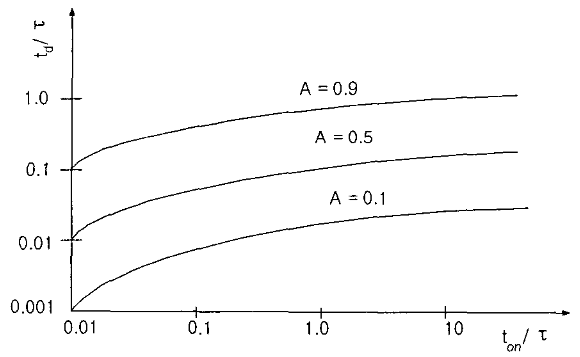

Fig. 7 Relationship between t_{on} and τ

Where A = V_s / V_B. The relation of t_d/τ can be shown in Fig. 7.

From Fig. 7, these two cases $t_{on}/\tau \ll 1$ and $t_{on}/\tau \gg 1$ should be different from equation (8) and equation (9).

$$t_d \simeq \frac{A}{1-A} t_{on} \qquad (t_{on}/\tau \ll 1) \tag{8}$$

$$t_d = \tau \cdot \ln\frac{1}{1-A} \qquad (t_{on}/\tau \gg 1) \tag{9}$$

The current i_L for continuous and discontinuous conditions is given by i_1 and i_2. The system circuit of Fig. 6 can be modeled by the following set of linear differential equations:

$$L\frac{di_L}{dt} = V_s - Ri_L \qquad \text{(on state)} \qquad (10)$$

$$L\frac{di_L}{dt} = V_s - V_B - Ri_L \qquad \text{(off state)} \qquad (11)$$

This converter has the function of a DC-DC boost switching regulator.

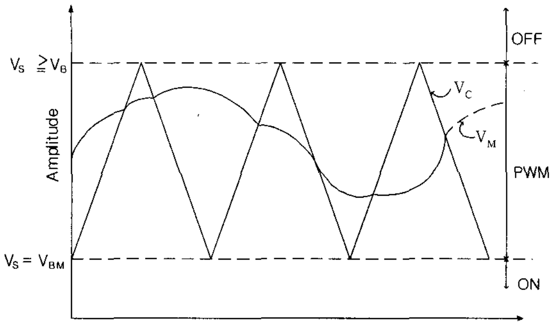

Fig. 8 Switching waveforms of converter

The converter switching strategy studied in this paper is a PWM algorithm. From Fig. 8, the PWM waveform for switching is generated by a modulating wave and a carrier wave. The generation of modulating signal V_M is produced by a difference voltage ($V_S - V_B$) for the switching condition. The carrier signal V_s is the T-periodic signal. The switching waveforms of the converter are seen in Fig. 8.

The converter switches from one state to another, whenever the generating voltage V_s is boosted under the control condition $V_{BM} \leq V_s \leq V_B$, where V_{BM} is a minimum battery voltage for switching condition.

The converter has three operating conditions, which are OFF, PWM and ON. As can be seen in Fig. 8, the operating condition of ON and OFF is fixed by V_s and V_B.

The switching condition is $V_C - V_M = 0$. The converter switches from on ($V_M \rangle V_C$) and off ($V_M \langle V_C$) in the PWM area. When the inductor current becomes zero during the off-state, the time is t_d ($\frac{di_L}{dt} = 0$). This converter algorithm includes the PWM strategy and the condition of t_d.

2.4 CB operation

The CB close signal for connecting the wind generator to the bus is produced by synchronizing conditions, such as voltage, frequency and phase. For this purpose, the wind generator voltage is maintained within ±3% of the bus voltage.

The output voltage would be 12Volt with 11m/sec wind speed. The CB control signal can be generated between 10m/sec to 14m/sec.

Synchronizing is performed with the wind generator frequency maintained at a high level compared with the bus frequency. In this paper, the CB signal for close is produced with the above condition.

3. Experimental Results

To verify the performance of the proposed hybrid system, the following parameters were selected for experimental implementation: The inductor L is 3mH, the capacitor C_S is $3000\,\mu F$, R is $3\,\Omega$.

From Fig. 9 (a), (b) and (c), the time evolution of the environmental condition can be observed. Fig. 9 (a) shows the wind speed signal varying between 6m/sec and 14m/sec, with a mean of 10.5m/sec. This waveform presents the turbulent part of the wind and its variation. The control signal of the CB is generated above 11m/sec. Fig. 9 (b) displays the current supply in the converter by the PV system. It can be seen that the PV power is a more static source than wind. Fig. 9 (c) shows the charge efficiency of wind generator and PV that it is estimated using the equation $\{i_L - (i_L - i_B)\} \times 100 / i_L$. The wind-PV hybrid system forms a complementary system and this complementary feature is favorable to system reliability.

The charge efficiency could be increased by way of a converter and the charging power fluctuation has been greatly reduced.

From Fig. 9 (d), the battery voltage maintains a constant voltage with the CB and the converter. The overvoltage was controlled by using the CB for the control output of the wind system. Also, the DC link fluctuation could be reduced by switching the strategy of the converter.

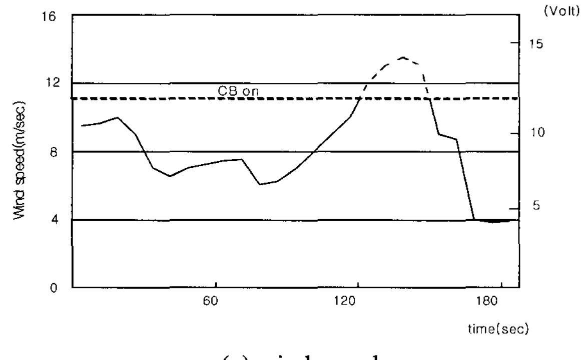

(a) wind speed

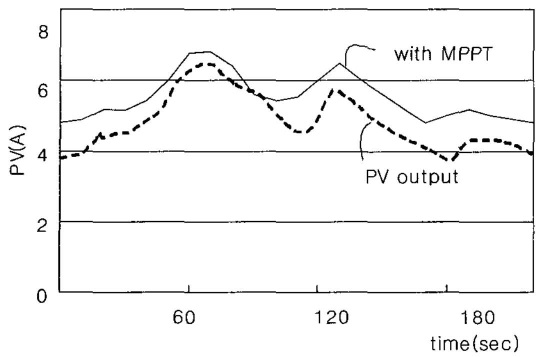

(b) outputs of PV system

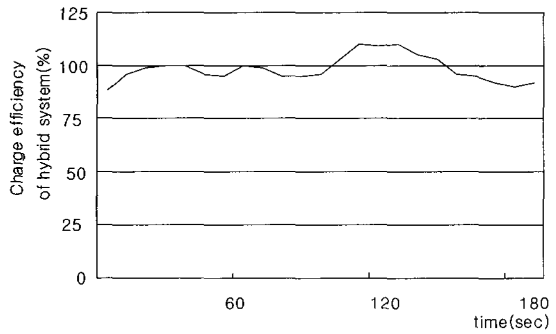

(c) charge efficiency of hybrid system

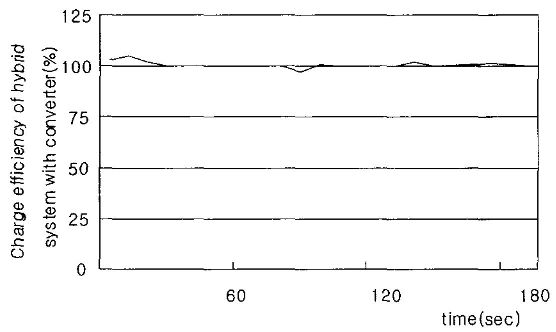

(d) charge efficiency of battery

Fig. 9 Experimental results

4. Conclusion

The wind-PV hybrid system forms a complementary system. Generally, solar power is a more static source than wind, but the wind provides energy during periods of no sunshine. This hybrid system has high levels of efficiency and reliability.

This paper describes a power control system with CB and converter. The overvoltage of the wind system is reduced by the CB and the DC link fluctuation is controlled via the converter. As such, DC bus fluctuation can be reduced with the CB and converter. Also, high efficiency power is achieved using the PWM strategy for the converter.

Acknowledgements

This paper was presented to the IFAC symposium (2003).

References

[1] Abdelali El Aroudi and Ramon Leyva (2001). Quasi-periodic route to Chaos in a PWM voltage -controlled DC-DC boost converter. *Circuits and systems-*, **Vol. 48,** pp. 967-977.

[2] Edurd Muljadi, Herbert L. Hess and Kim Thomas (2001). Zero sequence method for energy recovery form a variable-speed wind turbine generator. *Energy Conversion,* **Vol. 16,** pp. 99-103.

[3] Francois Giraud and Zyiad M. Salameh (2001). Steady-state performance of a grid-connected rooftop hybrid wind-photovoltaic power system with battery storage. *Energy Conversion,* **Vol. 16,** pp. 1-7.

[4] F. Valenciaga, P. F. puleston, P. E. Battaiotto and R. J. Mantz (2001). Passivity/sliding mode control of a stand-alone hybrid generation system. *Proc.-Control Theory,* **Vol. 147,** pp. 680-685.

[5] Gyu Bum Joung and Jae-Dong Choi, Design of Solar Array Simulator for Spaceecrsft, KIEE International Transactions on Electrical Machinery and Energy Conversion Systems, Vol. 12, No. 2, pp. 52-56, June, 2002

[6] Malinowski, Marian P. Kazmierkowski, Steffan Hansen, Frede Blaabjerg, G.D. Marques(2001). Virtual-flux-based direct power control of three-phase PWM rectifiers. *Industry Applications,* **Vol. 37, pp. 1010-1027.**

[7] Peng Wang and Roy Billinton (2001). Reliability benefit analysis of adding WTG to a distribution system. *Energy Conversion,* **Vol. 16,** pp. 134-139.

[8] P. S. Dokopoulos, A. C. Saramourtsis, A. G. Bakirtzis (1996). Prediction and evaluation of the performance of wind-diesel energy systems. *Energy Conversion,* **Vol. 11,** pp. 385-393.

[9] Z. Chen and E. Spooner(2001). Grid power quality with variable speed wind turbines. *Energy Conversion,* **Vol. 16,** pp. 148-153.

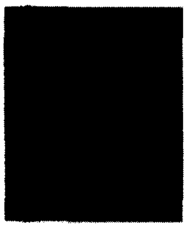

Jin-Seok Oh
He was born in Kyung-Nam, Korea. He received his B.E. degree in Marine Engineering from Korea Maritime University in 1983. After that, he was employed by Zodiac (England Company) where he was a System Engineer for four years. He received his M.E. and Ph.D. degrees from Korea Maritime University, Busan, Korea in 1989 and 1996, respectively. He was with the Agency for Defense Development (ADD) as a Researcher from 1989 to 1992. From 1992 to 1996, he was an Assistant Professor in the Department of Industrial Safety Engineering at Yangsan College. In 1996, he joined the Division of Mechatronics Engineering at Korea Maritime University. His research interests include electrical drive systems, robot control and PC-based control applications.

Ji-Young Lee
She was born in Chungnam, Korea. She received her Bachelor's degree in Marine Engineering from Korea Maritime University in 2002. Since 2002, she has been a graduate student at Korea Maritime University.